SCIENCE CHINA
Chemistry

•ARTICLES•

February 2024 Vol.67 No.2: 542–550
https://doi.org/10.1007/s11426-023-1794-2

Regioselective and asymmetric allylic alkylation of vinyl epoxides for the construction of allylic alcohols *via* synergistic catalysis

Min Chen[†], Longqing Yang[†], Yuzhen Li, Yinhe Qu, Guihua Pan, Xiaoming Feng[*] & Xiaohua Liu[*]

Key Laboratory of Green Chemistry & Technology, Ministry of Education, College of Chemistry, Sichuan University, Chengdu 610064, China

Received July 13, 2023; accepted September 6, 2023; published online November 17, 2023

A highly efficient asymmetric allylic alkylation of cyclic and acyclic carbon nucleophiles with vinyl epoxides has been developed, which exhibits good functional group compatibility, high atomic and step economy. This protocol utilizes a strategy of synergistic catalysis with a chiral *N*,*N*′-dioxide/Ni^{II} complex and an achiral Pd^0 catalyst, generating a series of multi-substituted allylic alcohols with a quaternary carbon stereocenter in high yield and excellent regio-, *Z*/*E*- and enantioselectivity under mild conditions. Further transformations of the product demonstrate the potential utility of this protocol in the synthesis of allyl alcohol derivatives and natural product analogues. Experimental studies revealed that the *N*,*N*′-dioxide/metal complexes play an important role in controlling the *Z*/*E*- and enantioselectivity. The density functional theory (DFT) calculations further demonstrated that multiple C–H···π interactions between the aromatic rings of the two substrates and the amide moiety in the ligand stabilized the dominant transition state.

asymmetric allylic alkylation, synergistic catalysis, vinyl epoxides, allyl alcohol, multiple weak interactions

Citation: Chen M, Yang L, Li Y, Qu Y, Pan G, Feng X, Liu X. Regioselective and asymmetric allylic alkylation of vinyl epoxides for the construction of allylic alcohols *via* synergistic catalysis. *Sci China Chem*, 2024, 67: 542–550, https://doi.org/10.1007/s11426-023-1794-2

1 Introduction

Transition-metal catalyzed asymmetric allylic alkylation (AAA) reaction (Tsuji-Trost allylation) has been developed into an efficient method for the construction of structurally diverse molecules bearing allylic substitutions [1]. The allylation reagents, including allyl halides, allyl alcohols, allyl carbonates, allyl carboxylates, and propene derivatives *via* allylic C–H oxidative functionalization as well, have been well studied with excellent achievements [2]. 1,3-Diene monoepoxide performs well atomic economy and reactivity as an allyl reagent [3], for it contains both double bond and strained oxirane, and the related zwitterionic π-allyl palladium intermediates [4] with various configuration are easily generated to act as versatile synthons in organic synthesis (Scheme 1a). In addition to acting as dipoles in cycloaddition reactions to furnish various heterocycles [5], vinyl epoxides undergo the AAA reaction to provide a potentially powerful approach to deliver allylic alcohols or homoallylic alcohols [6] (Scheme 1a). But if 2-substiuted vinyl epoxides are involved, the capture by nucleophiles seems to be more complicated, meeting the issues as branched or linear-selectivity (Scheme 1a, path (i) *vs*. paths (ii) and (iii)), *Z*- or *E*-selectivity (Scheme 1a, path (ii) *vs*. path (iii)), as well as enantioselectivity due to π-σ-π interconversion of π-allyl palladium species.

Previously, Trost's group [7] initiated the dynamic kinetic AAA of isoprene monoepoxide with β-ketoesters to perform the branched alkylation, giving the corresponding tetrahydrofurans as the major products (Scheme 1b, path (i)), and the regioselectivity is rationalized arising from the preferred

†These authors contributed equally to this work.
*Corresponding authors (email: xmfeng@scu.edu.cn; liuxh@scu.edu.cn)

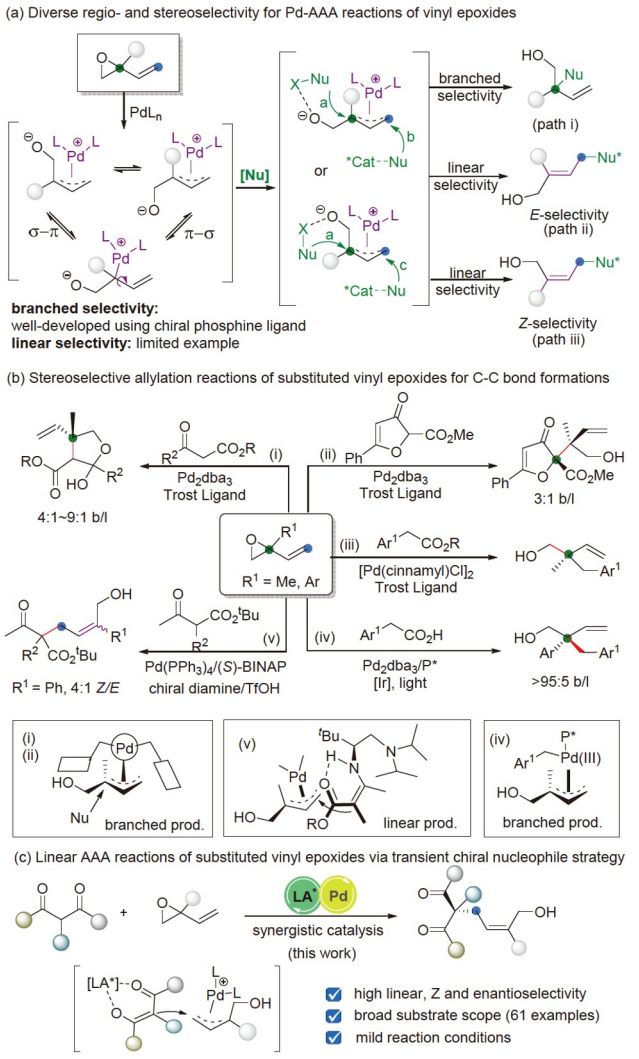

Scheme 1 The asymmetric allylic alkylation reactions of vinyl epoxides (color online).

alkylation of the DPPBA ligand-matched ionization of one enantiomer of isoprene monoepoxide. Taking advantage of Trost's Pd-AAA reaction, Xie and coworkers [8] realized the total synthesis of hyperolactone C and (−)-biyouyanagin A (Scheme 1b, path (ii)). Lundgren's *group* [9] accomplished the substitution of isoprene monoxide with arylacetates (Scheme 1b, path (iii)), and Yu and Zhang *et al*. [10] reported a decarboxylative allylic benzylation cocatalyzed by Pd/photoredox [Ir] to afford homoallylic alcohols (Scheme 1b, path (iv)). In most cases, branched homoallylic alcohols were furnished as the major products, and a linear-selective asymmetric allylic alkylation was reported by Luo's group [11] *via* a synergistic amine/palladium catalysis, but the strategy seemed to be suitable for alkyl β-ketocarbonyls, and one example of 2-subsitiuted vinyl epoxide was explored to give moderate *Z*/*E*-selectivity (Scheme 1b, path (v)). Though 1,4-addition to 1,3-diene epoxides has been known [11,12], the control of *Z*/*E*- and enantioselectivity of the reaction occurring at the terminal position is difficult with chiral palladium catalyst, due to several factors, such as the matched or unmatched interactions of racemic epoxide with ligand and the nucleophile, distant chiral environment of π-allyl palladium intermediate to the prochiral nucleophile, and fast interconversion of the intermediate species.

Based on our recent work on synergistic bimetallic catalysis in asymmetric catalysis [13], we found that chiral *N*,*N*′-dioxide/metal complexes have good compatibility with transition metal catalysts such as Au, Pd, Ir, and Rh. The chiral Lewis acids that differentiate the enantiotopic faces of the nucleophile, merging with the achiral palladium that promotes the formation of the zwitterionic intermediates, provides a new opportunity for the linear addition of various prochiral carbon nucleophiles to 1,3-diene monoepoxides (Scheme 1c). Herein, we report the combination of a chiral *N*,*N*′-dioxide/nickel complex and an achiral palladium catalyst which enables highly linear-, *Z*-, and enantioselective allylic alkylation of a series of cyclic and acyclic nucleophiles with vinyl epoxides. A wide variety of multi-substituted allylic alcohols bearing a quaternary carbon stereocenter were obtained with excellent activity and stereoselectivity (Scheme 1c). Density functional theory (DFT) calculations disclosed the origin of *Z*/*E*- and enantioselectivity of the synergistic catalysis.

2 Experimental

2.1 General procedure for the asymmetric reaction of vinyl epoxides and cyclic β-ketoamides/ketoesters

An oven-dried tube was charged with $Ni(OTf)_2$/**L_3-Pic*P*** (1:1, 10 mol%), **A** (0.10 mmol) under N_2 atmosphere. CH_2Cl_2 (1.0 mL) was added and the mixture was stirred at 35 °C for 30 min. Subsequently, $Pd(PPh_3)_4$ (1–2 mol%) and **B** (0.15 mmol) were added. The reaction was stirred at 35 °C and monitored by thin-layer chromatography (TLC). After completion, the reaction mixture was directly subjected to flash column chromatography on silica gel and eluted with petroleum ether/ethyl acetate to afford the corresponding product **C**.

2.2 General procedure for the asymmetric reaction of vinyl epoxides and acyclic β-ketoamides

An oven-dried tube was charged with $Ni(OTf)_2$/**L_3-Pic*H*** (1:1, 10 mol%), **D1**–**D11** (0.10 mmol) under N_2 atmosphere. CH_2Cl_2 (1.0 mL) was added and the mixture was stirred at 35 °C for 30 min. Subsequently, $Pd(PPh_3)_4$ (2 mol%), **B** (0.15 mmol) were added. The reaction was stirred at 35 °C and monitored by TLC. After completion, the reaction mixture was directly subjected to column chromatography on silica gel and eluted with petroleum ether/ethyl acetate to afford the corresponding product **E1**–**E11**.

2.3 General procedure for the asymmetric reaction of vinyl epoxides and aza-aryl acetamides/acetates

An oven-dried tube was charged with $Ni(OTf)_2$/**L_3-PiPr$_2$** (1:1, 10 mol%), **D12**–**D19** (0.10 mmol) under N_2 atmosphere. CH_2Cl_2 (1.0 mL) was added and the mixture was stirred at 35 °C for 30 min. Subsequently, $Pd(PPh_3)_4$ (1–2 mol%) and **B** (0.15 mmol) were added. The reaction was stirred at 35 °C and monitored by TLC. After completion, the reaction mixture was directly subjected to column chromatography on silica gel and eluted with petroleum ether/ethyl acetate to afford the corresponding products **E12**–**E19**.

3 Results and discussion

3.1 Optimization of the reaction conditions

In our initial investigation, we chose cyclic β-ketoamide **A1** and vinyl epoxide **B1** as the model substrates to optimize the reaction conditions (Table 1, see the Supporting Information online for details). The classic catalyst for allylic alkylation reaction as the complex of $Pd_2(dba)_3$ and Trost ligand **L1** promoted the reaction efficiently, and the linear product **C1** was afforded in high yield but with poor *Z*/*E* ratio and unsatisfactory enantioselectivity (entry 1). The catalyst of $[Ir(cod)Cl]_2$/(S_a,*S*,*S*)-**L2** gave only trace amount of product (entry 2). In comparison, the results in entries 3–5 demonstrated that the combination of achiral $Pd_2(dba)_3$/PPh_3 with chiral nickel complex of *N*,*N*′-dioxides dramatically affected both *Z*/*E*- and enantioselectivity, especially with the ligand **L_3-PiPr$_2$** derived from (*S*)-pipecolic acid, and up to 94% ee was achieved for the major *Z*-isomer (*Z*:*E* = 7.1:1; entry 5). Nevertheless, the dual-metallic catalysis led to reduced reactivities (see the Supporting Information online for details). The use of other Lewis acids, such as $Co(OTf)_2$, $Ni(OTf)_2$, and $Zn(OTf)_2$, afforded slightly increased yield, high enantioselectivity, and varied *Z*/*E* ratio, but $Cu(OTf)_2$ seemed less stereoselective (entry 9 *vs*. entries 6–8). In view of the high activity of $Pd(PPh_3)_4$ itself for racemic transformation (entry 10), we adjusted the combination by using $Pd(PPh_3)_4$ (1 mol%) to promote the generation of π-allyl palladium intermediate in order to increase the yield. As expected, a significant increase in yield (97% yield) with high *Z*/*E* ratio (>19:1 *Z*/*E*) was realized using $Pd(PPh_3)_4$ (1 mol%), while the enantioselectivity slightly decreased (81% ee; entry 11). In order to further improve the enantioselectivity, careful screening of the *N*,*N*′-dioxide ligands derived from (*S*)-pipecolic acid was carried out. It was found that **L_3-Pic*P*** was superior to other ligands, delivering the desired **C1** in 99% yield, >19:1 *Z*/*E*, 96% ee (Table 1, entry 12). Further increasing the steric hindrance of aliphatic amide moiety in the ligands, such as **L_3-PiAd**, led to a decrease in enantioselectivity and yield (entry 13). Attempt to reduce the amount of chiral catalyst resulted in slightly dropped *Z*/*E*- and enantioselectivity (Table 1, entry 14).

3.2 Substrate scope of cyclic β-ketoamides/ketoesters and vinyl epoxides

Under the optimized reaction conditions (Table 1, entry 12), the scope of cyclic β-ketoamides and β-ketoesters **A** was investigated firstly (Table 2). Various substituents at different positions on the inden-1-one-based β-ketoamides were tolerated to produce the desired linear-products (**C2**–**C20**) with good to excellent yields and enantioselectivities (82%–99% yields, 93%–98% ee). In general, the *Z*/*E*-selectivity for 4-, 7-substituted ones was higher (18:1–>19:1) than 5-, 6-substituted ones (7:1–19:1), the reduced *Z*/*E*-ratio was partly due to the increased amount of $Pd(PPh_3)_4$ (**C9**, **C14**–**C17**). Particularly, introducing functional groups, such as NO_2, CN, CF_3 had no obvious influence on enantioselectivity. Other cyclic ketoamides, including cyclopentanone-, 3,4-dihydronaphthalen-1(2H)-one-, and benzo[7]annulen-5-one-based ones could also participate in the allylation well, albeit the enantioselectivity dropped a little with larger ring (**C21**–**C23**). Furthermore, β-ketoamides bearing smaller or larger steric substituents on the amide moiety could also proceed smoothly to afford the corresponding products **C24**–**C26** in 85%–99% yields with 93%–97% ee. Besides, cyclic β-ketoesters were also amenable to the current reaction and exhibited excellent enantioselectivities (**C27**–**C32**, 95%–98% ee) in the presence of $Ni(OTf)_2$/**L_3-Pic*H*** catalyst instead of $Ni(OTf)_2$/**L_3-Pic*P*** (see the Supporting Information online for details). The *Z*/*E* configuration of the products is confirmed by both X-ray single crystal analysis and nuclear magnetic resonance (NMR) analysis. The absolute configuration of **C26** was determined to be (*Z*,*S*) based on X-ray crystallographic analysis [14a]. The configuration of other products was assigned by comparing their CD spectra with that of **C26** (see the Supporting Information online for details).

The alkylation of 2-aryl-2-vinyloxiranes **B** was explored with substitution at the aryl group, and the reactions performed well in terms of yield and enantioselectivity (**C33**–**C39**), while several products had a decreased *Z*/*E* ratio. The simple 2-vinyloxirane was amenable to this reaction, furnishing the corresponding product **C40** in 99 % yield, 1:2.2 *Z*/*E* ratio and 93%/94% ee. Methyl-substituted vinyl epoxide **B10** afforded the product **C41**–**C42** in good yield (93%–99% yields) and ee value (91%–98% ee). Noteworthily, high enantioselectivities were given for two *Z*/*E* isomers in the cases of low *Z*/*E*-selectivity, which showed that *Z*/*E*-selectivity was determined by both substrate and catalyst, and the enantioselectivity is under the control of the chiral Lewis acid. Overall, the presence of aromatic rings in both substrates is crucial for the high *Z*/*E*-selectivity of this reaction, and the

Table 1 Optimization of the reaction conditions [a)]

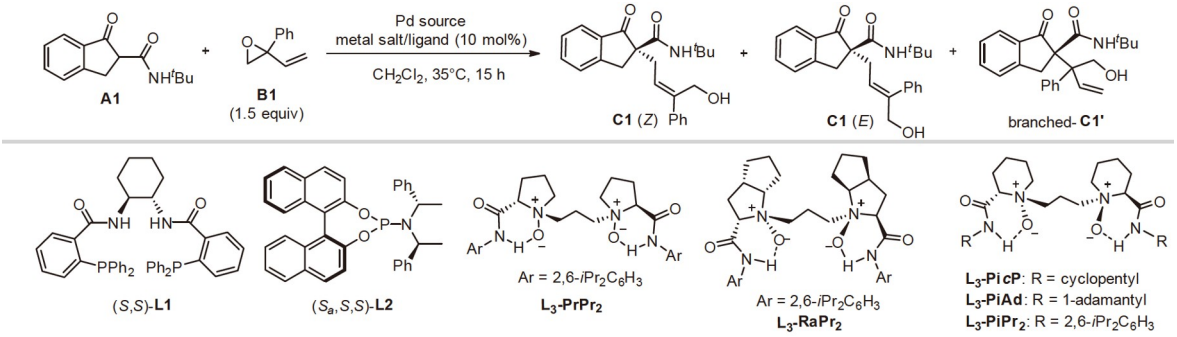

Entry	Catalyst	Yield [b)] (%)	*Z*/*E* [c)]	ee [d)] (%)
1	$Pd_2(dba)_3$/**L1** (1:2, 4 mol%)	93	1:1	22/70
2	$[Ir(cod)Cl]_2$/**L2** (1:2, 4 mol%)	Trace	–	–
3	$Pd_2(dba)_3$/PPh_3 (1:2, 2.5 mol%); $Ni(ClO_4)_2{\cdot}6H_2O$/**L_3-PrPr$_2$**	29	8.3:1	65
4	$Pd_2(dba)_3$/PPh_3 (1:2, 2.5 mol%); $Ni(ClO_4)_2{\cdot}6H_2O$/**L_3-RaPr$_2$**	63	>19:1	18
5	$Pd_2(dba)_3$/PPh_3 (1:2, 2.5 mol%); $Ni(ClO_4)_2{\cdot}6H_2O$/**L_3-PiPr$_2$**	27	7.1:1	94
6	$Pd_2(dba)_3$/PPh_3 (1:2, 2.5 mol%); $Co(OTf)_2$/**L_3-PiPr$_2$**	52	13.6:1	96
7	$Pd_2(dba)_3$/PPh_3 (1:2, 2.5 mol%); $Ni(OTf)_2$/**L_3-PiPr$_2$**	51	12.7:1	97
8	$Pd_2(dba)_3$/PPh_3 (1:2, 2.5 mol%); $Zn(OTf)_2$/**L_3-PiPr$_2$**	45	7.4:1	94
9	$Pd_2(dba)_3$/PPh_3 (1:2, 2.5 mol%); $Cu(OTf)_2$/**L_3-PiPr$_2$**	47	4.1:1	85
10	$Pd(PPh_3)_4$ (1 mol%)	99	2:1	0
11	$Pd(PPh_3)_4$ (1 mol%); $Ni(OTf)_2$/**L_3-PiPr$_2$**	97	>19:1	81
12	$Pd(PPh_3)_4$ (1 mol%); $Ni(OTf)_2$/**L_3-PicP**	99	>19:1	96
13	$Pd(PPh_3)_4$ (1 mol%); $Ni(OTf)_2$/**L_3-PiAd**	99	>19:1	87
14 [e)]	$Pd(PPh_3)_4$ (1 mol%); $Ni(OTf)_2$/**L_3-PicP**	99	15:1	96

a) Unless otherwise noted, all reactions were carried out with metal salt/Ligand (1:1, 10 mol%), PdL, **A1** (0.10 mmol) and **B1** (0.15 mmol) in CH_2Cl_2 (1.0 mL) at 35 °C for 15–24 h. b) Isolated yield. c) Determined by ^{1}H NMR. d) Determined by supercritical fluid chromatography (SFC) on a chiral stationary phase. e) $Ni(OTf)_2$/**L_3-PicP** (5 mol%).

Z/*E* ratio is significantly decreased when there are electron-withdrawing groups in the aromatic rings.

3.3 Substrate scope of acyclic β-ketoamides and aza-aryl acetamides/acetates

Subsequently, we turned our attention to investigate the compatibility of acyclic ketoamide substrates **D** (Table 3). After further condition optimization, various 2-fluoro-3-oxo-3-arylpropanamides were suitable as well in the presence of $Ni(OTf)_2$/**L_3-PicH** as the chiral catalyst (see the Supporting Information online for details). High *Z*/*E*-selectivity could be obtained based on the excellent isolated yield of *Z*-isomer *via* column chromatography separation, and enantioselectivities were also excellent for **E1**–**E8** (85%–95.5% ee). Moreover, 2-furanylcarbonyl and isobutyryl substitutions were also tolerable to afford the product **E9** with 98% yield, 99% ee, and **E10** in 87% yield and 82% ee, respectively. The reaction of 2-methyl vinyl epoxide performed smoothly to give *Z*/*E*-mixture product **E11** in 87% ee. Beyond that, a series of aza-aryl acetamides/acetates were also examined. It was found that different substituents on the aza-aryl ring were amenable to the present reaction, delivering the desired products **E12**–**E19** in excellent yields and enantioselectivities (85%–99% yields, 95%–99% ee). The absolute configurations of **E3** and **E12** were determined to be (*S*,*Z*) and (*R*,*Z*) based on X-ray crystallographic analysis [14b,14c], respectively.

3.4 Scale-up synthesis and further transformations of the products

To evaluate the synthetic potential of this protocol, the scale-up synthesis and some transformations of the products were carried out. As shown in Scheme 2a, vinyl epoxide **B1** can react with cyclic β-ketoamide **A26** (2.5 mmol) or acyclic azaaryl acetamide **D12** (3 mmol) under slightly modified

Table 2 Substrate scope of cyclic β-ketoamides/ketoesters and vinyl epoxides [a)]

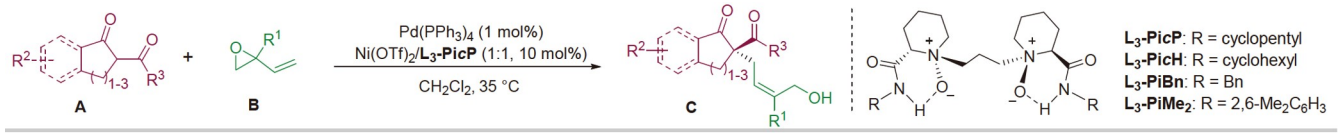

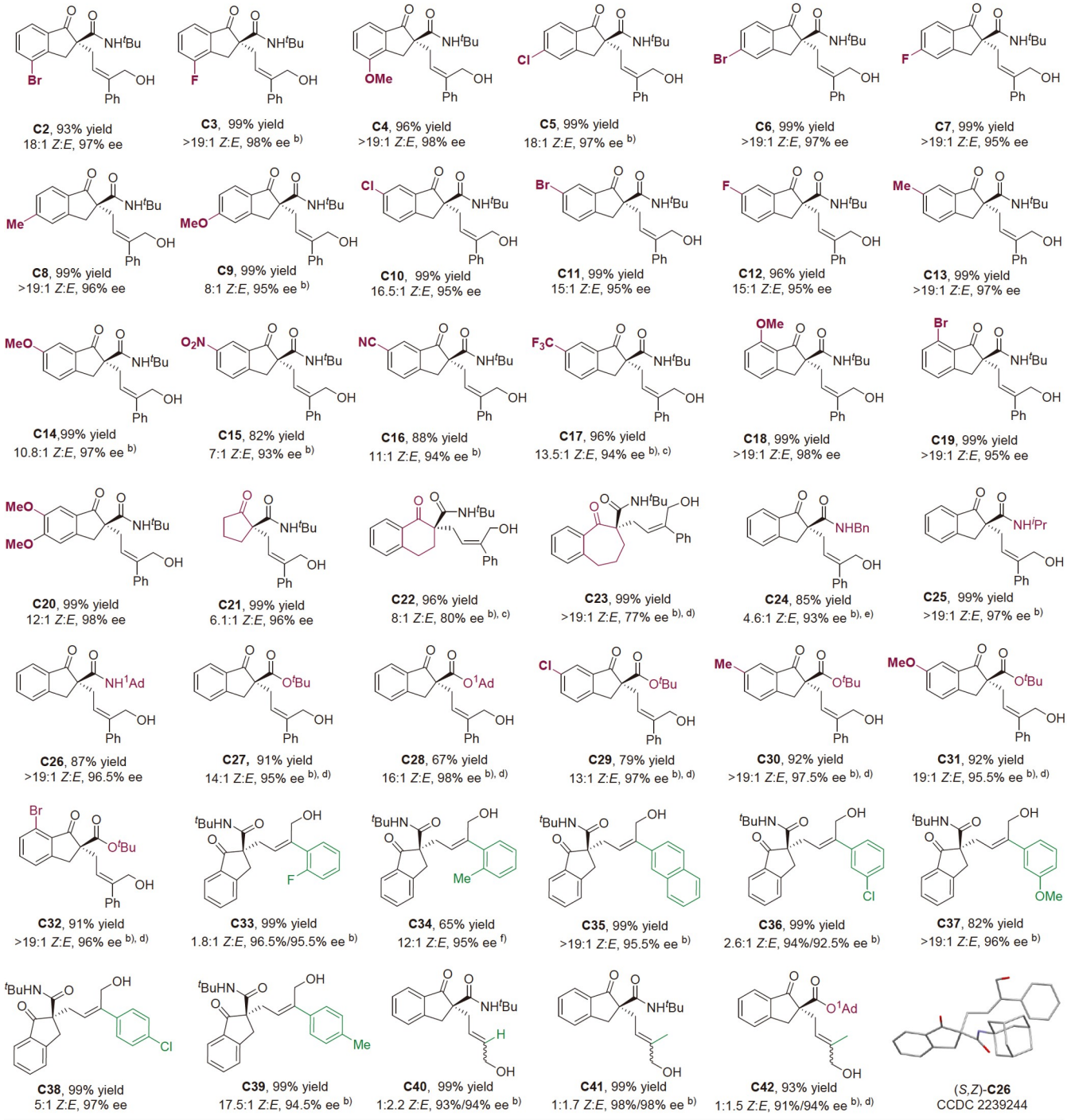

a) Unless otherwise noted, all reactions were carried out with Ni(OTf)$_2$/**L$_3$-PicP** (1:1, 10 mol%), Pd(PPh$_3$)$_4$ (1 mol%), **A** (0.10 mmol), and **B** (0.15 mmol) in CH_2Cl_2 (1.0 mL) at 35 °C for 24 h. b) Pd(PPh$_3$)$_4$ (2 mol%). c) **L$_3$-PiBn** (10 mol%). d) **L$_3$-PicH** (10 mol%). e) **L$_3$-PiMe$_2$** (10 mol%). f) Pd(PPh$_3$)$_4$ (5 mol%).

optimal conditions, providing the corresponding product **C26** or **E12** with nearly maintained yield and enantioselectivity. Several derivatizations of the allyl alcohol product **C26** were conducted (Scheme 2b). Firstly, Dess-Martin

Table 3 Substrate scope of acyclic β-ketoamides and aza-aryl acetamides/acetates [a]

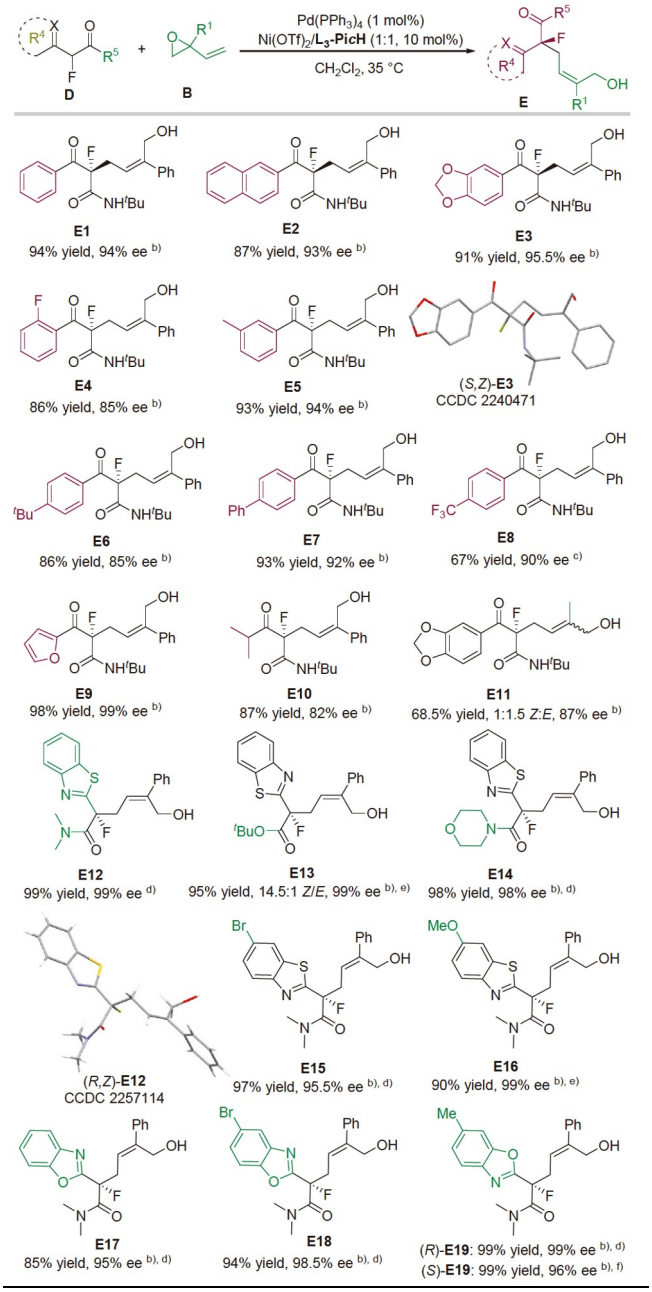

a) Unless otherwise noted, all reactions were carried out with $Ni(OTf)_2$/**L_3-PicH** (1:1, 10 mol%), $Pd(PPh_3)_4$ (1 mol%), **B** (0.15 mmol), and **D** (0.10 mmol) in CH_2Cl_2 (1.0 mL) at 35 °C for 24 h. Isolated yield of *Z*-isomer (without *Z*/*E* ratio) or *Z*/*E*-mixture (with *Z*/*E* ratio). b) $Pd(PPh_3)_4$ (2 mol%). c) $Pd(PPh_3)_4$ (5 mol%). d) **L_3-PiPr$_2$** (10 mol%). e) **L_3-PiMe$_2$** (10 mol%). f) *ent*-**L_3-PiPr$_2$** (10 mol%).

oxidation of **C26** generated α,β-unsaturated aldehyde **F1** in nearly equivalent yield. It could also be converted into an allylic imide **F2** in 79% yield *via* Mitsunobu reaction. Treatment with Pd/C and H_2 led to the formation of **F3** in 97% yield and 1:1 dr. Furthermore, epoxidation of **C26** with *m*-CPBA afforded **F4** in 92% yield and 1:1 dr. Surprisingly, when treating the product **E12** with *m*-CPBA, it was found

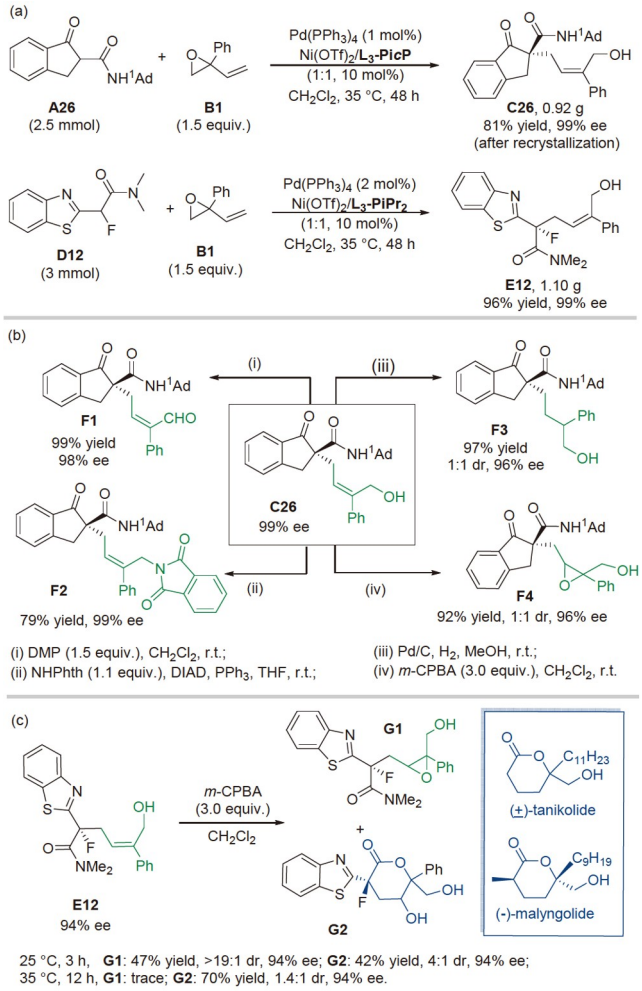

Scheme 2 (a–c) Scale-up synthesis and further transformations of the products (color online).

that not only epoxidation product **G1** but also a δ-lactone **G2** bearing a hydroxyl at C4 and a hydroxymethyl at C5 were produced (Scheme 2c). The skeleton structure of **G2** was similar to that of natural products as tanikolide and malyngolide [15]. And with increasing temperature and longer reaction time, **G1** could be completely converted to **G2** but the diastereoselectivity decreased. All these transformations could proceed smoothly with nearly maintained enantioselectivity.

3.5 Mechanism consideration and DFT calculations

Based on our previous research on the origin of stereoselectivity over dicarbonyl compounds by *N*,*N*′-dioxide/metal complex [16] and related work about palladium-catalyzed allylic alkylation reaction [13h], a possible synergistic catalytic mode is rationalized (Scheme 1c). On one hand, the chiral *N*,*N*′-dioxide and the bidentate nucleophilic substrate coordinates to $Ni(OTf)_2$ to form a catalyst-bonded enolate intermediate **INT1**. On the other hand, PdL_n^0 binds to the

double bond of vinyl epoxide to produce active *Z*/*E*-π-allylpalladium intermediates. There exists a π-σ-π interconversion process leading to variable *Z*/*E*-selectivity. Collectively, nucleophilic enolate intermediate **INT1** attacks the π-allylpalladium intermediate to give the desired product.

To understand the origin of regio-, *Z*/*E*- and enantioselectivity in the process, we carried out DFT calculations using chiral *N*,*N*′-dioxide **L_3-PicP** in the formation of the product **C1** at the solvation model density (SMD) [17a] (dichloromethane) M06L [17b]/def2-tzvpp [17c]//M06L/def2-svp [17c], SDD (Ni, Pd) [17d,17e] level (Figure 1). For the purpose of enhancing convenience and saving computing costs, $Pd(PPh_3)_4$ has been substituted with $Pd(PCH_3)_4$ in this study. An empirical van der Waals correction on DFT (DFT-D3) was adopted [17f]. All computations were performed using the Gaussian 09 software [18].

The results indicated that the formation of (*S*,*Z*)-**C1** is kinetically and thermodynamically more favorable than other configurations due to the lower free energy of the transition state (*S*,*Z*)-**TS** and the intermediate (*S*,*Z*)-**INT2**. Analysis of the weak interactions [19] in (*S*,*Z*)-**TS** and (*S*,*E*)-**TS** show that there are multiple stabilizing interactions in (*S*,*Z*)-**TS**, including the C–H···π interaction between the benzene ring of vinyl epoxide and C–H bond on cyclopentyl of **L_3-PicP**, the O–H···π interaction between the hydroxyl group of the π-allylpalladium intermediate and the fused benzene ring of **A1**, which is in agreement with the experimental findings that the presence of aromatic rings in both substrates is crucial for high *Z*/*E*-selectivity (**C21** and **C40**), but aromatic ring bearing electron-withdrawing group can weaken these stabilizing interactions resulting in a decreased *Z*/*E*-selectivity (**C15-C17**, **C33**, **C36**, and **C38**). Obviously, in (*S*,*E*)-**TS**, there are more steric repulsions and only one stabilizing C–H···π interaction (see the Supporting Information online for details).

With related to the enantioselectivity, we analysed the attack of the *Z*-π-allylpalladium intermediate on the *Re* and *Si* faces of the α-position of cyclic β-ketoamide **A1**, resulting in (*S*,*Z*)-**INT2** and (*R*,*Z*)-**INT2**, respectively. The energy of the corresponding transition state (*S*,*Z*)-**TS** *via* *Re*-face attack is much lower than that of (*R*,*Z*)-**TS**, indicating that the product is almost exclusively *S*-configuration. Analysis of the weak interactions (see the Supporting Information online for details) vividly explains this process: the lack of C–H···π interaction and partial steric hindrance make the energy higher, forming a non-dominant reaction pathway. The *E*-π-allyl-

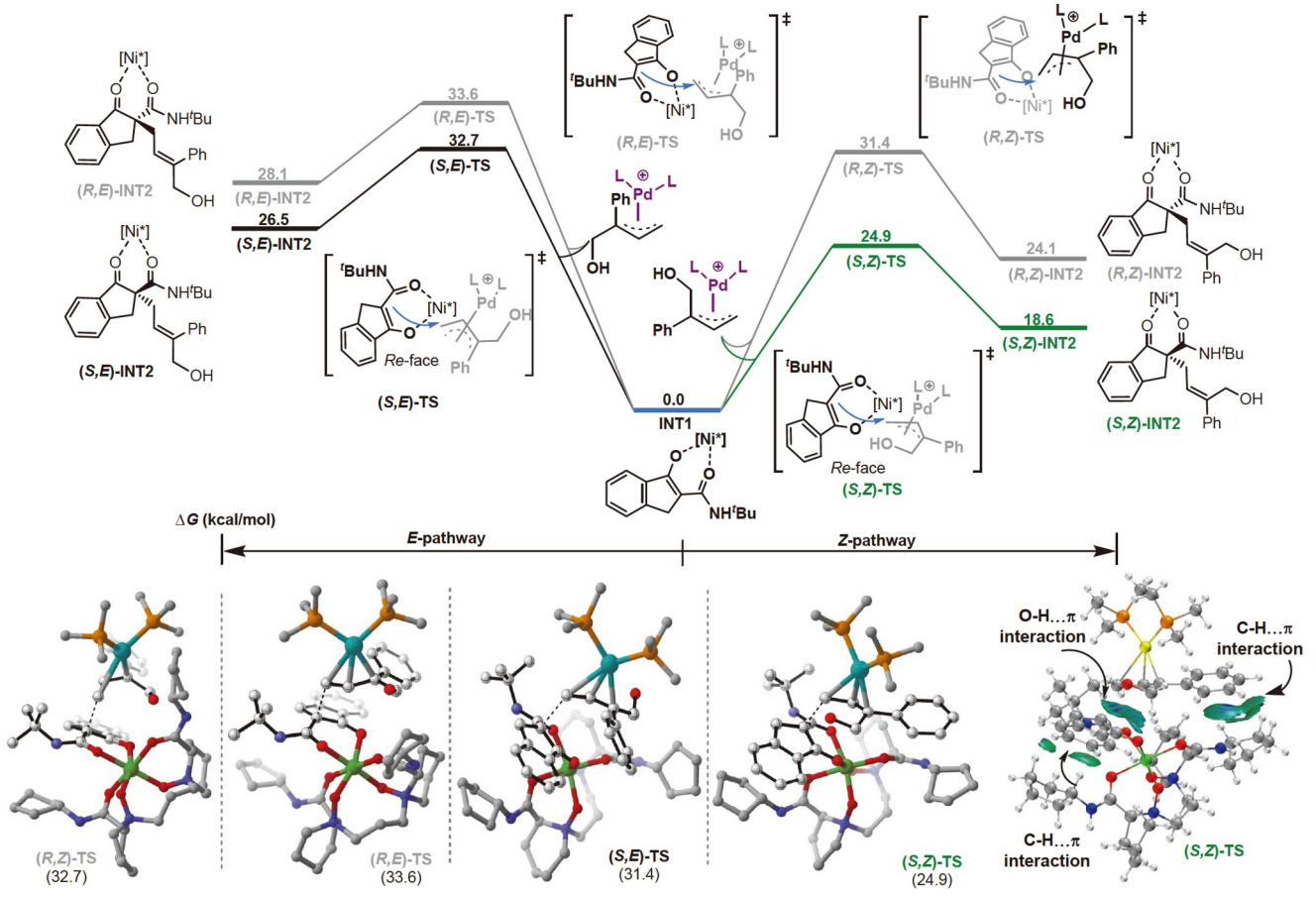

Figure 1 Calculated relative Gibbs free energy of regio- and asymmetric allylic alkylation of **A1** and **B1** with SMD (dichloromethane), M06L/def2-tzvpp//M06L/def2-svp; SDD (Co) level of theory. The free energy barriers ($\Delta G^{\ddagger}$) are given in kcal/mol (color online).

palladium intermediate on the *Re* and *Si* faces of the α-position of cyclic β-ketoamide **A1** also yields similar results. In addition, the reaction process of 2-methyl substituted vinyl epoxide **B10** was calculated as well (see the Supporting Information online for details). The relatively lower energy barrier difference is also consistent with the poor *Z*/*E* ratio in the experimental results.

4 Conclusions

In conclusions, we have developed a highly efficient asymmetric allylic alkylation of a series of cyclic and acyclic carbon nucleophiles with vinyl epoxides. Based on the combination of the *N*,*N*′-dioxide/Ni^{II} complex with Pd^0 catalyst, the corresponding multisubstituted allylic alcohols bearing a quaternary carbon stereocenter were obtained in high yield and excellent regio-, *Z*/*E*- and enantioselectivity. The scale-up synthesis and further transformations of the products showed that this protocol has potential utility in the synthesis of allyl alcohol derivatives and natural product analogues. DFT calculations showed that there are multiple stabilizing C–H···π and O–H···π interactions in the dominant transition state (*S*,*Z*)-**TS**, which further proved that *Z*/*E*-selectivity was determined by both substrate and catalyst, and the enantioselectivity was under the control of the *N*,*N*′-dioxide/metal complexes. The method represents a useful compensative route for asymmetric allylic alkylation and is expected to be used for other asymmetric reactions.

Acknowledgements This work was supported by the National Natural Science Foundation of China (U19A2014) and Sichuan University (2020SCUNL204). We are grateful to Dr Yuqiao Zhou (Sichuan University) for the X-ray single crystal diffraction analysis.

Conflict of interest The authors declare no conflict of interest.

Supporting information The supporting information is available online at http://chem.scichina.com and http://link.springer.com/journal/11426. The supporting materials are published as submitted, without typesetting or editing. The responsibility for scientific accuracy and content remains entirely with the authors.

1 (a) Trost BM, Crawley ML. *Chem Rev*, 2003, 103: 2921–2944; (b) Trost BM, Machacek MR, Aponick A. *Acc Chem Res*, 2006, 39: 747–760; (c) Trost BM, Fandrick DR. *ChemInform*, 2008, 39: 59–72; (d) Lu Z, Ma S. *Angew Chem Int Ed*, 2008, 47: 258–297; (e) Liu Y, Han SJ, Liu WB, Stoltz BM. *Acc Chem Res*, 2015, 48: 740–751; (f) Süsse L, Stoltz BM. *Chem Rev*, 2021, 121: 4084–4099; (g) Pàmies O, Margalef J, Cañellas S, James J, Judge E, Guiry PJ, Moberg C, Bäckvall JE, Pfaltz A, Pericàs MA, Diéguez M. *Chem Rev*, 2021, 121: 4373–4505; (h) Wei L, Wang CJ. *Chem Catal*, 2023, 3: 100455; (i) Wang PS, Gong LZ. *Chin J Chem*, 2023, 41: 1841–1848

2 (a) Trost BM, Thaisrivongs DA, Donckele EJ. *Angew Chem Int Ed*, 2013, 52: 1523–1526; (b) Lin HC, Wang PS, Tao ZL, Chen YG, Han ZY, Gong LZ. *J Am Chem Soc*, 2016, 138: 14354–14361; (c) Hu RB, Wang CH, Ren W, Liu Z, Yang SD. *ACS Catal*, 2017, 7: 7400–7404; (d) Rieckhoff S, Meisner J, Kästner J, Frey W, Peters R. *Angew Chem Int Ed*, 2018, 57: 1404–1408; (e) Matsui JK, Gutiérrez-Bonet Á, Rotella M, Alam R, Gutierrez O, Molander GA. *Angew Chem Int Ed*, 2018, 57: 15847–15851; (f) Fan LF, Luo SW, Chen SS, Wang TC, Wang PS, Gong LZ. *Angew Chem Int Ed*, 2019, 58: 16806–16810; (g) Lin HC, Xie PP, Dai ZY, Zhang SQ, Wang PS, Chen YG, Wang TC, Hong X, Gong LZ. *J Am Chem Soc*, 2019, 141: 5824–5834; (h) Zhang J, Yang WL, Zheng H, Wang Y, Deng WP. *Angew Chem Int Ed*, 2022, 61: e202117079; (i) Jiang R, Zhao QR, Zheng C, You SL. *Nat Catal*, 2022, 5: 1089–1097; (j) Xiao L, Chang X, Xu H, Xiong Q, Dang Y, Wang CJ. *Angew Chem Int Ed*, 2022, 61: e202212948; (k) Tian K, Chang X, Xiao L, Dong XQ, Wang CJ. *Fundamental Res*, 2022, doi: 10.1016/j.fmre.2022.07.008; (l) Higashida K, Smaïl V, Nagae H, Carpentier JF, Mashima K. *ACS Catal*, 2023, 13: 2156–2161; (m) Qi J, Song T, Yang Z, Sun S, Tung CH, Xu Z. *ACS Catal*, 2023, 13: 2555–2564; (n) Nilova A, Mannchen MD, Noel AN, Semenova E, Grenning AJ. *Chem Sci*, 2023, 14: 2755–2762; (o) Ke M, Yu Y, Sun L, Li X, Cao Q, Xiao X, Chen F. *Chem Commun*, 2023, 59: 2632–2635

3 (a) Marshall JA. *Chem Rev*, 1989, 89: 1503–1511; (b) He J, Ling J, Chiu P. *Chem Rev*, 2014, 114: 8037–8128; (c) Du Q, Zhang L, Gao F, Wang L, Zhang W. *Chin J Org Chem*, 2022, 42: 3240–3262; (d) Xu J, Song Y, He J, Dong S, Lin L, Feng X. *Angew Chem Int Ed*, 2021, 60: 14521–14527; (e) Xu J, Song Y, Yang J, Yang B, Su Z, Lin L, Feng X. *Angew Chem Int Ed*, 2023, 62: e202217887

4 (a) Niu B, Wei Y, Shi M. *Org Chem Front*, 2021, 8: 3475–3501; (b) Yang C, Yang ZX, Ding CH, Xu B, Hou XL. *Chem Record*, 2021, 21: 1442–1454

5 (a) Shaghafi MB, Grote RE, Jarvo ER. *Org Lett*, 2011, 13: 5188–5191; (b) Liu Z, Feng X, Du H. *Org Lett*, 2012, 14: 3154–3157; (c) Ma C, Huang Y, Zhao Y. *ACS Catal*, 2016, 6: 6408–6412; (d) Cheng Q, Zhang HJ, Yue WJ, You SL. *Chem*, 2017, 3: 428–436; (e) Suo JJ, Du J, Liu QR, Chen D, Ding CH, Peng Q, Hou XL. *Org Lett*, 2017, 19: 6658–6661; (f) Cheng Q, Zhang F, Cai Y, Guo YL, You SL. *Angew Chem Int Ed*, 2018, 57: 2134–2138; (g) Wang YN, Yang LC, Rong ZQ, Liu TL, Liu R, Zhao Y. *Angew Chem Int Ed*, 2018, 57: 1596–1600; (h) Peng Y, Huo X, Luo Y, Wu L, Zhang W. *Angew Chem Int Ed*, 2021, 60: 24941–24949; (i) Sarkar T, Talukdar K, Das BK, Shah TA, Debnath B, Punniyamurthy T. *Org Biomol Chem*, 2021, 19: 3776–3790

6 (a) Trost BM, Bunt RC, Lemoine RC, Calkins TL. *J Am Chem Soc*, 2000, 122: 5968–5976; (b) Trost BM, Tang W, Schulte JL. *Org Lett*, 2000, 2: 4013–4015; (c) Miyashita M, Mizutani T, Tadano G, Iwata Y, Miyazawa M, Tanino K. *Angew Chem Int Ed*, 2005, 44: 5094–5097; (d) Alibés R, Bayón P, de March P, Figueredo M, Font J, García-García E, González-Gálvez D. *Org Lett*, 2005, 7: 5107–5109; (e) Raghunath M, Zhang X. *Tetrahedron Lett*, 2005, 46: 8213–8216; (f) Trost BM, Zhang T. *Org Lett*, 2006, 8: 6007–6010; (g) Hale KJ, Manaviazar S, George JH, Walters MA, Dalby SM. *Org Lett*, 2009, 11: 733–736; (h) Mangion I, Strotman N, Drahl M, Imbriglio J, Guidry E. *Org Lett*, 2009, 11: 3258–3260; (i) Li G, Feng X, Du H. *Org Biomol Chem*, 2015, 13: 5826–5830; (j) Hu W, Lin Z, Wang C. *Org Lett*, 2022, 24: 5751–5755

7 Trost BM, Jiang C. *J Am Chem Soc*, 2001, 123: 12907–12908

8 Du C, Li L, Li Y, Xie Z. *Angew Chem Int Ed*, 2009, 48: 7853–7856

9 Doyle MGJ, Gabbey AL, McNutt W, Lundgren RJ. *Angew Chem Int Ed*, 2021, 60: 26495–26499

10 Song C, Zhang HH, Yu S. *ACS Catal*, 2022, 12: 1428–1432

11 Wang Y, Chai J, You C, Zhang J, Mi X, Zhang L, Luo S. *J Am Chem Soc*, 2020, 142: 3184–3195

12 (a) Trost BM, Molander GA. *J Am Chem Soc*, 1981, 103: 5969–5972; (b) Tsuji J, Kataoka H, Kobayashi Y. *Tetrahedron Lett*, 1981, 22: 2575–2578

13 (a) Zhang X, You R, Wei Z, Jiang X, Yang J, Pan Y, Wu P, Jia Q, Bao Z, Bai L, Jin M, Sumpter B, Fung V, Huang W, Wu Z. *Angew Chem Int Ed*, 2020, 59: 7969; (b) Hu B, Zhang X, Mo Y, Li J, Lin LL, Liu X, Feng X. *Org Lett*, 2020, 22: 1034–1039; (c) Dong P, Chen L, Yang Z,

Dong S, Feng X. *Org Chem Front*, 2021, 8: 6874–6880; (d) Xu C, Qiao J, Dong S, Zhou Y, Liu X, Feng X. *Chem Sci*, 2021, 12: 5458–5463; (e) Wang K, Xu C, Hu X, Zhou Y, Lin L, Feng X. *Chem Commun*, 2021, 57: 8917–8920; (f) Lang J, Wang S, He C, Liu X, Feng X. *Chem Sci*, 2022, 13: 1163–1168; (g) Liu Y, Chen Y, Yihuo A, Zhou Y, Liu X, Lin L, Feng X. *ACS Catal*, 2022, 12: 1784–1790; (h) Wang H, Xu Y, Zhang F, Liu Y, Feng X. *Angew Chem Int Ed*, 2022, 61: e202115715; (i) Wang W, Zhang F, Liu Y, Feng X. *Angew Chem Int Ed*, 2022, 61: e202208837; (j) Xu Y, Wang HK, Yang Z, Zhou YQ, Liu YB, Feng XM. Chem, 2022, 8: 2011–2022

14 (a) CCDC 2239244 (**C26**); (b) CCDC 2240471 (**E3**); (c) CCDC 2257114 (**E12**)

15 (a) Singh IP, Milligan KE, Gerwick WH. *J Nat Prod*, 1999, 62: 1333–1335; (b) Carda M, Rodrıguez S, Castillo E, Bellido A, Dıaz-Oltra S, Alberto Marco J. *Tetrahedron*, 2003, 59: 857–864; (c) Doran R, Duggan L, Singh S, Duffy CD, Guiry PJ. *Eur J Org Chem*, 2011, 2011: 7097–7106; (d) Jinnouchi H, Nambu H, Fujiwara T, Yakura T. *Tetrahedron*, 2018, 74: 1059–1070

16 (a) Liu XH, Lin LL, Feng XM. *Acc Chem Res*, 2011, 44: 574–587; (b) Liu X, Zheng H, Xia Y, Lin L, Feng X. *Acc Chem Res*, 2017, 50: 2621–2631; (c) Wang M-, Li W. *Chin J Chem*, 2021, 39: 969–984; (d) Dong S, Liu X, Feng X. *Acc Chem Res*, 2022, 55: 415–428; (e) Liu Y, Liu X, Feng X. *Chem Sci*, 2022, 13: 12290–12308; (f) Chen DF, Gong LZ. *Org Chem Front*, 2023, 10: 3676–3683; (g) Zhang X, Wu W, Cao W, Yu H, Xu X, Liu X, Feng X. *Angew Chem Int Ed*, 2020, 59: 4846–4850; (h) Hu X, Tang X, Zhang X, Lin L, Feng X. *Nat Commun*, 2021, 12: 3012; (i) He C, Wu Z, Zhou Y, Cao W, Feng X. *Org Chem Front*, 2022, 9: 703–708; (j) Wang Y, Yihuo A, Wang L, Dong S, Feng X. *Sci China Chem*, 2022, 65: 546–553; (k) Zhan T, Yang L, Chen Q, Weng R, Liu X, Feng X. *CCS Chem*, 2023, 5: 2101–2110; (l) Wu Z, Zhang X, Xu N, Liu X, Feng X. *ACS Catal*, 2023, 13: 815–823

17 (a) Marenich AV, Cramer CJ, Truhlar DG. *J Phys Chem B*, 2009, 113: 6378–6396; (b) Zhao Y, Schultz NE, Truhlar DG. *J Chem Theor Comput*, 2006, 2: 364–382; (c) Weigend F, Ahlrichs R. *Phys Chem Chem Phys*, 2005, 7: 3297–3305; (d) Andrae D, Häußermann U, Dolg M, Stoll H, Preuß H. *Theoret Chim Acta*, 1990, 77: 123–141; (e) Jensen F. *J Chem Theor Comput*, 2006, 2: 1360–1369; (f) Grimme S. *J Comput Chem*, 2006, 27: 1787–1799

18 Frisch MJ, Trucks GW, Schlegel HB, Scuseria GE, Robb MA, Cheeseman JR, Scalmani G, Barone V, Mennucci B, Petersson GA, Nakatsuji H, Caricato M, Li X, Hratchian HP, Izmaylov AF, Bloino J, Zheng G, Sonnenberg JL, Hada M, Ehara M, Toyota K, Fukuda R, Hasegawa J, Ishida M, Nakajima T, Honda Y, Kitao O, Nakai H, Vreven T, Montgomery Jr JA, Peralta JE, Ogliaro F, Bearpark M, Heyd JJ, Brothers E, Kudin KN, Staroverov VN, Kobayashi R, Normand J, Raghavachari K, Rendell A, Burant JC, Iyengar SS, Tomasi J, Cossi M, Rega N, Millam JM, Klene M, Knox JE, Cross JB, Bakken V, Adamo C, Jaramillo J, Gomperts R, Stratmann RE, Yazyev O, Austin AJ, Cammi R, Pomelli C, Ochterski JW, Martin RL, Morokuma K, Zakrzewski VG, Voth GA, Salvador P, Dannenberg JJ, Dapprich S, Daniels AD, Farkas Ö, Foresman JB, Ortiz JV, Cioslowski J. Fox DJ. Gaussian09, Revision D.01. Wallingford, CT: Gaussian, Inc., 2013

19 (a) Lu T, Chen F. *J Comput Chem*, 2012, 33: 580–592; (b) Lu T, Chen Q. *J Comput Chem*, 2022, 43: 539–555